



HAL
open science

Electroreforming of glucose/xylose mixtures on PdAu based nanocatalysts

Thibault Rafaideen, Stève Baranton, Christophe Coutanceau

► **To cite this version:**

Thibault Rafaideen, Stève Baranton, Christophe Coutanceau. Electroreforming of glucose/xylose mixtures on PdAu based nanocatalysts. *ChemElectroChem*, 2022, 9 (2), pp.e202101575. 10.1002/celec.202101575 . hal-03516506

HAL Id: hal-03516506

<https://cnrs.hal.science/hal-03516506>

Submitted on 7 Sep 2022

HAL is a multi-disciplinary open access archive for the deposit and dissemination of scientific research documents, whether they are published or not. The documents may come from teaching and research institutions in France or abroad, or from public or private research centers.

L'archive ouverte pluridisciplinaire **HAL**, est destinée au dépôt et à la diffusion de documents scientifiques de niveau recherche, publiés ou non, émanant des établissements d'enseignement et de recherche français ou étrangers, des laboratoires publics ou privés.

Electroreforming of glucose/xylose mixtures on PdAu based nanocatalysts

Thibault Rafaïdeen^[a], Stève Baranton^[a] and Christophe Coutanceau^{*[a,b]}

[a] Dr., TR, Rafaïdeen, Dr., SB, Baranton, Prof., CC, Coutanceau
Institut de Chimie des Milieux et Matériaux de Poitiers
CNRS – Université de Poitiers
4 rue Michel Brunet, TSA 51106, 86073 Poitiers cedex 9, France
E-mail: christophe.coutanceau@univ-poitiers.fr

[b] Prof., CC, Coutanceau
French Research Network on Hydrogen (FRH2), CNRS, France

Supporting information for this article is given via a link at the end of the document

Abstract: The electro-reforming of glucose/xylose mixtures has been evaluated at Pd_{1-x}Au_x/C anodes in 0.10 mol L⁻¹ NaOH electrolyte. The catalysts synthesized by a wet chemistry route are comprehensively characterized by physicochemical and electrochemical techniques. From linear scan voltammetry and *in-situ* Fourier transform infrared spectroscopy measurements, it was shown that the Pd_{0.3}Au_{0.7}/C material led to the best electrocatalytic behavior towards the electrooxidation of glucose/xylose mixtures in terms of activity (higher current densities at lower potentials) and selectivity (lower dissociative adsorption). Six-hour chronoamperometry measurements were performed at 293 K in a 25 cm² electrolysis cell at +0.4 V and +0.6 V and the reaction products were analyzed by high performance liquid chromatography. The main products were gluconate and xylonate, but the contributions of xylose to the whole products formed was always lower in percentages than the initial xylose ratios in solutions, showing that glucose was more electro-reactive than xylose at Pd_{0.3}Au_{0.7} surface.

Introduction

The electro-conversion of oxygenated compounds from biomass is now considered as an interesting mean for the simultaneous production of both value-added compounds at the anode and hydrogen at the cathode of an electrolysis cell^[1,2]. Lignocellulosic biomass is a very abundant non-edible raw material that has attracted huge interest in bio-refineries for production of fuels and chemicals^[3]. According to the feedstock, lignocellulosic biomass contains 30 - 45 % cellulose, 20 - 50 % hemicellulose and around 20 % lignin^[4]. Lignin is composed of an amorphous heteropolymer network of phenyl propane units held together by different linkages and has interest for second generation biofuel production. Cellulose is a linear crystalline polymer composed of glucose units^[4] linked via β-(1,4) glycosidic bonds, whereas hemicelluloses are branched polymers of mainly pentoses (xylose, arabinose) and hexoses (mannose, glucose, galactose)^[5]. In fact, glucose and xylose are the main sugars in hydrolysates after lignocellulosic biomass pretreatments to separate lignin from carbohydrates, and it has been proposed that the economically feasible production of valuable chemicals from lignocellulosic biomass should also lean on the conversion of both xylose and glucose^[6].

The carboxylic acid (carboxylate) derivatives of glucose and xylose, gluconic (gluconate) and xylonic (xylonate) acids,

respectively, are of great interest as bio-sourced platform molecules^[7] for a large panel of applications^[8,9]. We recently showed that each of these sugars could be electrooxidized with very high conversion rate and selectivity into their corresponding carboxylate form using carbon supported alloyed Pd_{1-x}Au_x/C (atomic ratios, with 0 ≤ x ≤ 1) nanostructured materials, with the Pd_{0.3}Au_{0.7}/C one leading to the higher catalytic performances^[10].

The objective of the present contribution is to evaluate the electrocatalytic behavior of such materials towards the electrooxidation of mixtures of glucose and xylose. Considering that cellulose and hemicellulose are each present at about the same ratio in lignocellulosic biomass (see above), that cellulose contains only hexoses, and that hemicellulose contains both pentoses and hexoses^[11], the electrocatalytic behaviors of Pd_{1-x}Au_x/C materials will be studied in alkaline aqueous glucose/xylose mixtures with molar ratios 90%/10%, 70%/30% and 50%/50% and compared to those for pure glucose and xylose solutions. Chronoamperometry measurements will be performed using the most promising anodic catalysts to check its behavior in a two electrode electro-reforming reactor. To our knowledge, this is the first time that such a study on the evaluation of the electrochemical reactivity of glucose/xylose mixtures is proposed.

Results

Physicochemical characterization of catalysts

The Pd_{1-x}Au_x/C catalysts were characterized by physicochemical and electrochemical methods in a previous work^[10]. Table 1 summarizes the main physicochemical and electrochemical characteristics of materials. The actual metal loadings (*W*) were determined by thermogravimetric analyses (TGA), whereas the Pd/Au atomic ratios (comp.) were estimated from atomic absorption spectroscopy (AAS). The good agreement between the actual and nominal metal loadings and atomic ratios indicated that the synthesis was quantitative, e.g., all metal ions were integrated in the catalytic nanoparticles.

The values of particle sizes (d_{TEM}) from transmission electron spectroscopy (TEM) images and crystallite sizes (L_v) from x-ray diffraction (XRD) pattern analyses followed the same trends, i.e., increasing with the increase of the Au content in nanoparticles (NPs). From XRD pattern analyses, the lattice parameter (*a*) has been shown to linearly increase with the Au content, which

confirmed the formation of PdAu alloy structures. From electrochemical measurements, it was shown that the surface of Pd_{1-x}Au_x nanoparticles was palladium rich compared to the bulk composition for $x = 0.7$, exhibiting only Pd and a single PdAu surface alloy, whereas for $x = 0.3$ the catalyst exhibited two PdAu surface alloys of different compositions coexisting with pure gold islands. In addition, the electroactive surface area of the catalysts (ESA) decreased with the gold content from ca. 60 m² g_{metal}⁻¹ for Pd/C to ca. 14 m² g_{metal}⁻¹ for Au/C.

Table 1. Main physicochemical and electrochemical characteristics of Pd_{1-x}Au_x/C catalysts by TGA (*W*), AAS (comp.), XRD (*a* and *L_v*), TEM (*d_{TEM}*) and cyclic voltammetry (alloy surface comp., total surface comp. and ESA).

	Pd/C	Pd _{0.7} Au _{0.3} /C	Pd _{0.3} Au _{0.7} /C	Au/C
<i>W</i> (wt%)	40.0	36.2	41.3	35.4
Comp. (at%)	Pd: 100 Au: 0	Pd: 80 Au: 20	Pd: 23 Au: 77	Pd: 0 Au: 100
<i>a</i> (Å)	3.897	3.936	4.033	4.071
<i>L_v</i> (nm)	2.9	3.3	5.9	4.4
<i>d_{TEM}</i> (nm)	4.0	4.3	5.8	6.8
Surface alloy comp. (at%)	Pd: 100 Au: 0	Pd: 89 Au: 11	Pd: 81 60 0 Au: 19 40 100	Pd: 0 Au: 10 0
Total surface comp. (at%)	Pd: 100 Au: 0	Pd: 89 Au: 11	Pd: 28 Au: 72	Pd: 0 Au: 100
ESA (m ² g _{metal} ⁻¹)	61	33	20	14

Electrocatalytic evaluation of Pd_{1-x}Au_x/C materials

The electrocatalytic behaviors of the Pd_{1-x}Au_x/C materials are first investigated by comparing for each glucose/xylose ratio in the electrolyte (with a total concentration of glucose and xylose of 0.10 mol L⁻¹) the third stable LSVs recorded on all catalysts at the scan rate of 0.005 V s⁻¹ from +0.050 V to +1.200 V vs RHE in 0.10 mol L⁻¹ NaOH electrolyte (Figure 1). Because the current densities are corrected from the metal loadings as determined by TGA, LSVs in Figures 1 and 2 compare the mass activity of catalysts as a function of the electrode potential for the oxidation of different glucose/xylose ratios in the electrolyte.

The first remark is that Pd and Au behave differently for aldose electrooxidation, gold being more active than palladium in the low potential region as higher current densities are recorded on Au/C than on Pd/C from ca. +0.200 V to ca. +0.600 V vs RHE for glucose oxidation and from ca. +0.250 V to ca. +0.720 V vs RHE for xylose oxidation. This could be due to a lower gold surface poisoning by species from aldose adsorption than on Pd surface. The second remark is that xylose seems less electro-reactive than glucose at low potentials as the onset potential of oxidation (defined as the potential for which the current density reaches a value of 0.15 mA cm⁻²) is always higher for xylose electrooxidation than for glucose electrooxidation, independently on the Pd_{1-x}Au_x/C catalyst composition.

But the most important result from this study is that the Pd_{0.3}Au_{0.7}/C catalyst displays the lowest onset potential of oxidation and the highest achieved current densities in the

potential region from +0.100 V to +0.500 V vs RHE, whatever the glucose/xylose molar ratio is. The higher tolerance to poisoning of a non-alloyed Pd_{0.3}Au_{0.7}/C catalyst amongst a series of Pd_{1-x}Au_x/C materials was already pointed out by Yan et al.^[12] for the electrooxidation of pure glucose in alkaline medium. Rafaideen et al.^[10] found that the alloyed Pd_{0.3}Au_{0.7}/C catalyst also presented the higher tolerance to poisoning for both pure glucose and pure xylose electrooxidation in alkaline medium. It is now generalized to glucose/xylose mixtures.

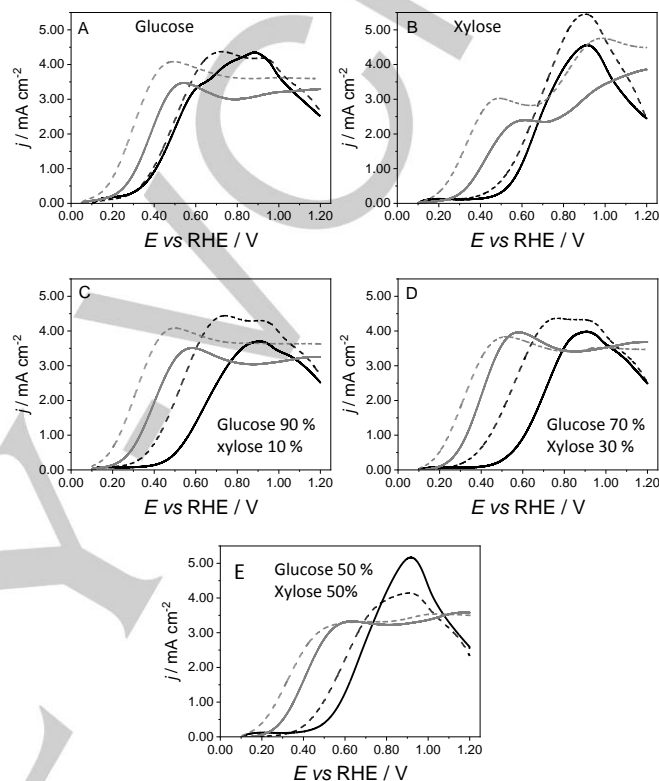


Figure 1. Linear scan voltammetry recorded on Pd/C (plain black line), Pd_{0.7}Au_{0.3}/C (dashed black line), Pd_{0.3}Au_{0.7}/C (dashed grey line) and Au/C (plain grey line) for the electrooxidation of (A) 0.10 mol L⁻¹ glucose, (B) 0.10 mol L⁻¹ xylose, (C) 0.10 mol L⁻¹ glucose 90%/xylose 10%, (D) 0.10 mol L⁻¹ glucose 70%/xylose 30% and (E) 0.10 mol L⁻¹ glucose 50%/xylose 50%. Scan rate = 0.005 V s⁻¹, N₂-purged 0.10 mol L⁻¹ NaOH electrolyte, *T* = 293 K).

Pd/C and Au/C catalysts do not behave similarly towards the electrooxidation of aldoses, and Au/C is more active than Pd/C. But when both metals are alloyed, a synergistic effect emerges that makes the onset potential for the oxidation of pure xylose, pure glucose and glucose/xylose mixtures shifting towards lower values than those of pure metals; the Pd_{0.3}Au_{0.7} atomic composition allows achieving the lowest onset potentials.

To better visualize the electrocatalytic consequences of this synergistic effect, Figure 2 compares the third stable LSVs recorded on each Pd_{1-x}Au_x/C catalyst for the oxidation of different glucose/xylose ratios in the electrolyte.

Considering first the Pd/C catalyst (Figure 2A), the onset potential for glucose electrooxidation is +0.300 V vs RHE and shifts towards higher values with the increase of xylose molar ratio in the mixture, to reach +0.350 V vs RHE and +0.400 V vs

RHE for glucose/xylose molar ratios of 90%/10% and 70%/30%, respectively, indicating a competition for adsorption/oxidation of both molecules at the Pd surface. It is worth to note that for a glucose/xylose molar ratio of 50%/50%, the LSV almost completely superimposes that recorded in pure xylose solution. These results may indicate that xylose has higher affinity for the Pd surface than glucose and that the adsorption of xylose leads to more strongly adsorbed species that need higher electrode potentials to be removed from the catalyst surface. The same trend can be observed for the palladium-rich surface Pd_{0.7}Au_{0.3}/C catalyst without pure gold islands (Figure 2B).

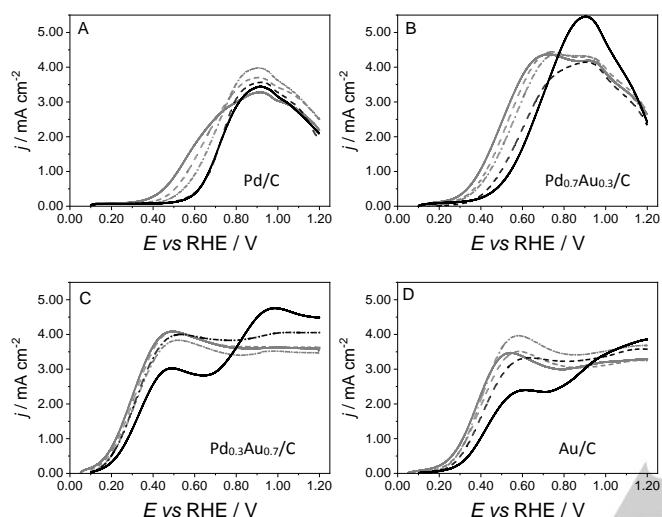


Figure 2. Linear scan voltammetry recorded for the electrooxidation of 0.10 mol L⁻¹ glucose (plain grey line), 0.10 mol L⁻¹ xylose (plain black line), 0.10 mol L⁻¹ glucose 90%/xylose 10% (dashed grey line), 0.10 mol L⁻¹ glucose 70%/xylose 30% (dashed-dotted grey line) and 0.10 mol L⁻¹ glucose 50%/xylose 50% (dashed black line) on (A) Pd/C, (B) Pd_{0.7}Au_{0.3}/C, (C) Pd_{0.3}Au_{0.7}/C and (D) Au/C. Scan rate = 0.005 V s⁻¹, N₂-purged 0.10 mol L⁻¹ NaOH electrolyte, T = 293 K.

The Pd_{0.3}Au_{0.7}/C catalyst, that displays pure gold islands together with two PdAu surface alloys, led to LSV shapes for the electrooxidation of glucose/xylose mixtures (Figure 2C) differing drastically from those recorded on Pd-rich catalysts and resembling those recorded on the monometallic Au/C material (Figure 2D). The increase of the xylose molar ratio from 10% to 50% does not involve significant changes in the shape of the LSV and in the electrooxidation onset potentials, which remain close to that of glucose oxidation on Au/C catalyst, as if glucose had higher affinity than xylose with such gold-rich surfaces. Pd_{0.3}Au_{0.7}/C catalyst is not only the most active catalyst in terms of lower electrooxidation onset potentials and higher current densities in the potential range from +0.150 V to +0.700 V vs RHE, but also seems to be more tolerant to the presence of xylose up to 50% molar ratio as all polarization curves are closer each to the others from the electrooxidation onset potential to ca. +0.400 V vs RHE than in the case of other catalyst compositions.

In situ infrared investigation of the electrooxidation of glucose/xylose mixtures

To obtain some insights on the behavior of catalysts towards the electrooxidation of pure glucose, pure xylose, glucose 90%/xylose 10% and glucose 50%/xylose 50% mixtures, *in situ* infrared spectra were recorded on Pd/C, Pd_{0.3}Au_{0.7}/C and Au/C materials (Figure 3).

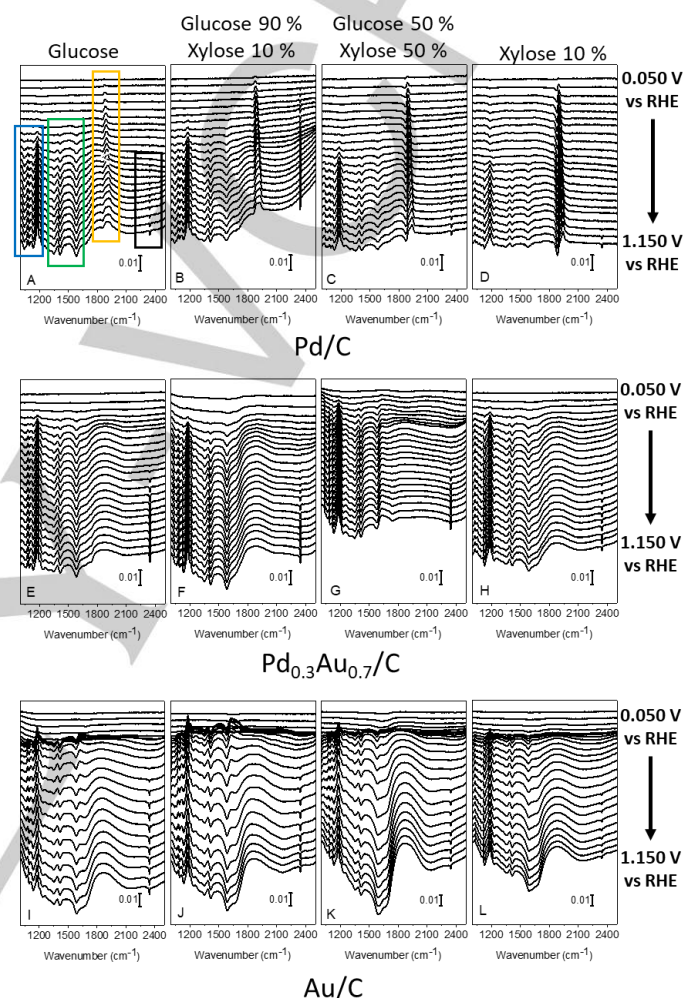


Figure 3. Infrared spectra recorded from +0.050 to +1.150 V vs RHE for the electrooxidation on (A,B,C,D) Pd/C, (E,F,G,H) Pd_{0.3}Au_{0.7}/C and (I,J,K,L) Au/C of (A,E,I) 0.10 mol L⁻¹ glucose, (B,F,J) 0.10 mol L⁻¹ glucose 90%/xylose 10%, (C,G,K) 0.10 mol L⁻¹ glucose 50%/xylose 50% and (D,H,L) 0.10 mol L⁻¹ xylose. Scan rate: 0.001 V s⁻¹, resolution 4 cm⁻¹, N₂-purged 0.10 mol L⁻¹ NaOH electrolyte, T = 293 K. Vertical scale: $\Delta R/R$. In Figure 3A, the blue box highlights the C-O stretching region¹³, the green one the bands from O-C-O vibration modes, the orange one the CO_{ads} band and the black one the interfacial CO₂ band.

Regarding the spectra recorded on Pd/C (Figures 3A, B, C, D), they all exhibit about the same absorption bands. Four negative bands are located at ca. 1060, 1099, 1137 and 1225 cm⁻¹ and a positive one at ca. 1176 cm⁻¹, i.e. in the C-O stretching region^[13].

Then, two negative bands at ca. 1417 and 1587 cm^{-1} assigned to symmetric and asymmetric stretching mode of O-C-O, and a band at ca. 1357 cm^{-1} assigned to the $\delta(\text{O-C-O})$ vibration mode correspond to the formation of carboxylates^[13,14]. These observations imply that same chemical groups are reacting and formed for the electrooxidation of pure glucose, pure xylose and mixtures of glucose/xylose on Pd/C catalyst. A strong absorption band shifts between 1890 and 1940 cm^{-1} with the applied electrode potential. This band is assigned to the formation of adsorbed bridge-bonded carbon monoxide species (CO_{ads}) on palladium^[15]. Therefore, the palladium surface can break the C-C bond and perform the dissociative adsorption of aldoses from very low electrode potentials. The shift in the position of this band (ca. 42.5 cm^{-1}/V) can be due to both the Stark effect induced by the electrode potential and the change in dipole-dipole interaction between CO_{ads} species with the variation of the surface coverage^[16].

It is worth to notice that the relative intensity between the negative adsorption bands in the 1000 to 1700 cm^{-1} wavenumber region and the bridged CO_{ads} band decreases gradually with the increase of the xylose molar ratio in the electrolyte. This observation indicates that the Pd surface coverage by bridged CO_{ads} increases also gradually with the xylose molar ratio, confirming the higher affinity of xylose towards Pd surface than glucose and a higher surface poisoning by xylose than by glucose. At last, a negative band growth with electrode potential at 2343 cm^{-1} corresponding to the formation of interfacial CO_2 ^[17].

Now, regarding the *in situ* infrared spectra recorded on $\text{Pd}_{0.3}\text{Au}_{0.7}/\text{C}$ (Figures 3 E, F, G, H) and Au/C (Figures 3 I, J, K, L) catalysts, the same absorption bands as in the case of Pd/C are exhibited in the 1000 to 1700 cm^{-1} wavenumber range. Therefore, same chemical functions are either reacting (positive band) or formed (negative bands). But, in these cases no band corresponding to adsorbed CO species is observed. The CO_2 band starts to be observed from +0.700 V vs RHE. This means that, at least for electrode potential lower than +0.650 V vs RHE, no C-C bond breaking occurs and therefore that gluconate and/or xylonate are produced on the Au surface-rich $\text{Pd}_{0.3}\text{Au}_{0.7}/\text{C}$ (presenting Au islands) and Au/C catalysts. However, due to the very low changes in recorded spectra with the glucose/xylose molar ratio in electrolytes, no indication on the higher affinity of glucose or xylose towards these catalytic surfaces can be obtained from these experiments.

Chronoamperometry measurements

To obtain supplementary information on the behavior of the $\text{Pd}_{0.3}\text{Au}_{0.7}/\text{C}$ catalyst towards electro-reforming of glucose/xylose mixtures, chronoamperometry measurements were first performed for 6 hours at a cell voltage of +0.4 V (anode potentials corresponding to the first oxidation wave in LSV) and 25 °C, and the reaction products analyzed every hour by high performance liquid chromatography. The experimental set-up, analytical methods and data treatment were explained elsewhere^[10,18,19]. The cathodic counter reaction being the hydrogen evolution reaction (HER), it has been shown previously that the anode potential remained between +0.35 V and +0.40 V vs RHE^[10,18]. Because LSVs point out the following trend in terms of current achieved for electrode potentials lower than +0.4 V vs. RHE, glucose 90%/xylose 10% > glucose 70%/xylose 30% > glucose 50%/xylose 50%, the chronoamperometry measurements were performed for glucose

90%/xylose 10% (Figure 4A) and glucose 50%/xylose 50% (Figure 4B) mixtures in 0.10 mol L⁻¹ NaOH aqueous electrolyte. In both cases, the formation of gluconate and xylonate increases with time. The percentages of gluconate and xylonate formed are always close to the initial percentages of glucose and xylose in the electrolytes, as if both sugars reacted simultaneously at the catalyst surface with the same kinetics.

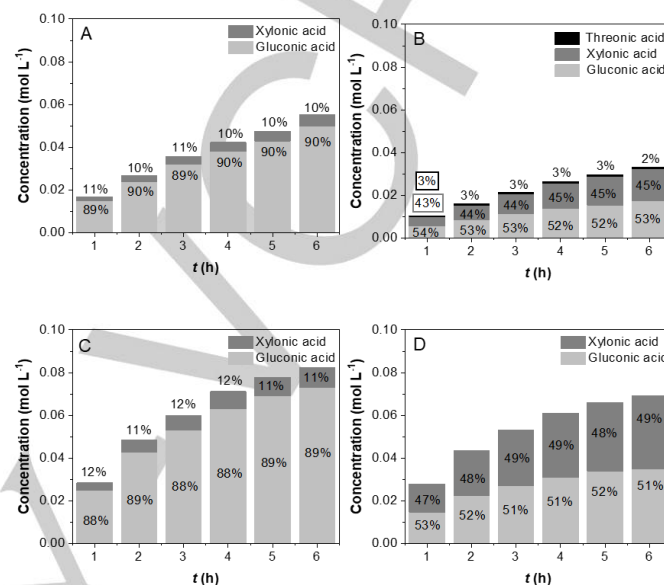


Figure 4. Histograms of product distribution (gluconic, xylonic and threonic acids) as a function of time determined by HPLC from 600 μL aliquots sampled every hour of chronoamperometry measurements for 6 hours at 293 K for the electro-reforming of (A, C) 0.10 mol L⁻¹ glucose 90%/xylose 10% and (B, D) 0.10 mol L⁻¹ glucose 50%/xylose 50% at cell voltages of (A,B) +0.4 V and (C, D) +0.6 V.

However, it is worth to notice that the faradaic charges recorded are lower in the chronoamperometry measurements performed from the glucose 50%/xylose 50% mixture than from the glucose 90%/xylose 10% one (Table 2 and Figure SI1 in Supporting Information). At the same time, the amount of gluconate and xylonate formed decreases from 0.0553 mol L⁻¹ (0.0500 mol L⁻¹ gluconate and 0.0053 mol L⁻¹ xylonate) in the case of electro-reforming of glucose 90%/xylose 10% mixture to 0.0333 mol L⁻¹ (0.0175 mol L⁻¹ gluconate, 0.0149 mol L⁻¹ xylonate) in the case of electroreforming of glucose 50%/xylose 50% mixture. In addition, a very small amount of threonate (0.0009 mol L⁻¹ threonate) could be determined in the last case.

Chronoamperometry measurements at a cell voltage of +0.6 V (as for the cell voltage of +0.4 V, it can be expected that the anode potential lies in the range from +0.50 V to +0.60 V vs RHE, which corresponds to potentials in the oxidation current plateau in LSV) displayed the same trends as at +0.4 V, i.e., the percentages of gluconate and xylonate formed were always close to the initial percentages of glucose and xylose in the electrolyte (Figures 4D and 4E), but the faradaic charges recorded are only slightly lower from the glucose 50 xylose 50% mixtures than from the glucose 90%/xylose 10% one (Table 2,

and Figure S11 in Supporting Information). But the conversion rates of glucose and xylose are higher at +0.6 V than at +0.4 V as higher charges and concentrations of gluconate and xylonate were obtained, with 0.0824 and 0.0690 mol L⁻¹ for glucose 90%/xylose 10% and glucose 5%/xylose 50%, respectively, at +0.6 V against 0.0553 and 0.0324 mol L⁻¹, respectively, a +0.4 V. Note that for such a cell voltage, no threonate could be detected by HPLC.

Table 2. Data from the electroreforming of glucose 90 %/xylose 10 % and glucose 50 %/xylose 50 % determined from HPLC analysis of the reaction products.

	glucose 90 %/xylose 10 %		glucose 50 %/xylose 50 %	
Cell voltage (V)	+0.4	+0.6	+0.4	+0.6
C _{gluconate} (mol L ⁻¹) ^a	0.0500	0.0730	0.0175	0.035
C _{xylonate} (mol L ⁻¹) ^a	0.0053	0.0094	0.0149	0.034
C _{threonate} (mol L ⁻¹) ^a	0	0	0.0009	0
C _{products}	0.0553	0.0824	0.0333	0.069
% gluconate	90.4	88.6	52.5	50.1
% xylonate	9.6	11.4	44.7	49.7
% threonate	0	0	2.8	0
X	0.35	0.44	0.21 (y = 0) 0.27 (y = 1)	0.69
Glucose contribution (%)	96.7	95.	90.6 (y = 0) 87.9 (y = 1)	66.0
Xylose contribution (%)	3.3	5.0	9.4 (y = 0) 12.1 (y = 1)	34.0

Discussion

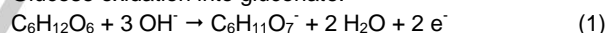
On the one hand, LSV measurements indicate that xylose can be less reactive than glucose at the Pd and Au based catalytic surface as higher onset potentials and lower current densities from the onset potential of oxidation to ca. +0.500 V vs RHE are recorded. On the other hand, infrared spectroscopy measurements clearly indicate that on Pd rich surfaces, xylose undergoes strong dissociative adsorption from very low electrode potentials forming more adsorbed CO species than glucose, according to the relative intensities of the infrared band in the 1900 cm⁻¹ region. Therefore, one could conclude that xylose is not less reactive than glucose on Pd rich surface, but more prone to dissociatively adsorb and poison the surface and to block it for further reactions. However, for gold-rich surfaces, i.e., in the case of the Pd_{0.3}Au_{0.7}/C and Au/C catalysts, the dissociative adsorption of xylose seems to be avoided or at least limited since no CO absorption band was observed on the infrared spectra. Elsewhere, it was proposed that the formation of close-packed vertically adsorbed gluconic or xylonic molecules was responsible of the gold surface deactivation (poisoning)^[20]. But the LSVs of xylose electrooxidation on Pd_{0.3}Au_{0.7}/C display higher onset potentials and lower current densities in the region of potentials lower than +0.5 V vs RHE,

speaking towards either a lower reactivity of xylose compared with that of glucose or to a higher adsorption strength of the xylose adsorbed intermediate (xylonate) than that of the glucose one (gluconate).

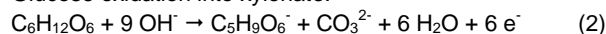
Results from chronoamperometry measurements at a cell voltage of +0.4 V indicate that the increase of xylose proportion in the anolyte leads to a decrease of the electrical charges involved in the electroreforming reaction (Table 2). Chromatograms from HPLC (Figure S11 in Supporting Information) display highly intense peaks related to gluconic and xylonic acids, as well as very small peaks (almost not observable from the background) corresponding to threonic, glycolic and formic acids, indicating that those last products are formed as traces. The fact that glucose oxidation produces gluconate together with ca. 9.3 mol % xylonate and traces of threonate after 6 hours electroreforming of 0.10 mol L⁻¹ glucose in 0.10 mol L⁻¹ NaOH electrolyte at a Pd_{0.3}Au_{0.7}/C catalyst at a cell voltage of +0.4 V was already evidenced in a previous work^[10]. The C2 and C1 species are likely produced during the oxidation processes of glucose into xylonate and threonate, and of xylose into threonate. Therefore, the conversion rate decreases also with the xylose concentration in the electrolyte. However, according to HPLC measurements, the ratios of xylonate and gluconate after 6 hours of chronoamperometry at +0.4 V and +0.6 V are very close to those of xylose and glucose in the mother mixtures, which could be explained by a similar reactivity of both aldoses and a similar reaction rate into their corresponding carboxylate forms.

It is also worth to notice that the peak at ca. 8.6 min assigned to threonate¹⁹ is only hardly visible in the chromatograms (Figure S11 in Supporting Information) for the electroreforming of the glucose 50%/xylose 50% mixture at +0.4 V and absent to those from the other reaction media. Considering the formation of only carbonate as by-product, the oxidation reaction involved at the anode of the electro-reforming cell to produce gluconate, xylonate and threonate are the following:

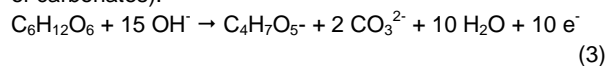
Glucose oxidation into gluconate:



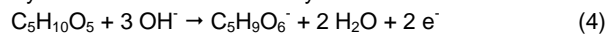
Glucose oxidation into xylonate:



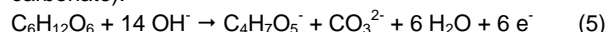
Glucose oxidation into threonate (considering only co-formation of carbonates):



Xylose electrooxidation into xylonate:



Xylose oxidation into threonate (considering only co-formation of carbonate):



Because xylonate and threonate can be formed from both glucose and xylose electrooxidation reactions, it is not possible to determine the faradaic efficiencies by comparing the actual electrochemical charges involved in the chronoamperometry measurements and the theoretical ones calculated from the amounts of formed compounds as determined by HPLC. However, looking at the chromatograms in Supporting Information (Figures S12, S13 and S14), no other product than gluconic, xylonic and threonic acids was significantly detected. As explained above, the possible traces of C2 and C1 can be formed when glucose is oxidized into xylonate and threonate,

and xylose into threonate. At last, the cell voltages at which the reactions are studied (+0.4 V and +0.6 V) are low enough to discard any possibility of oxygen evolution reaction (that occurs at cell voltages higher than 1.23 V^[21]). Therefore, it can reasonably be considered that all the electrical charges involved in the chronoamperometry measurements are coming from the electrooxidation of glucose and xylose into gluconate, xylonate and threonate.

From the possible electrochemical semi-reactions, a mathematical equation that links the total electrical charges (Q) involved in the electroreforming process to the concentrations of gluconate ($C_{\text{gluconate}}$), xylonate (C_{xylonate}) and threonate ($C_{\text{threonate}}$) formed can be proposed:

$$Q = FV(2C_{\text{gluconate}} + 2xC_{\text{xylonate}} + 6(1-x)C_{\text{xylonate}} + 6yC_{\text{threonate}} + 10(1-y)C_{\text{threonate}}) \quad (6)$$

$$Q = 2FV(C_{\text{gluconate}} + 3C_{\text{xylonate}} - 2xC_{\text{xylonate}} - 2yC_{\text{threonate}} + 5C_{\text{threonate}}) \quad (7)$$

where, F is the Faraday constant ($F = 96,485 \text{ C mol}^{-1}$), V is the volume of anolyte electro-reformed ($V = 0.030 \text{ L}$), x ($0 \leq x \leq 1$) is the proportion of xylose used to produce xylonate considering equation (4) and y ($0 \leq y \leq 1$) is the proportion of xylose used to produce threonate according to equation (5), 2 is the number of electrons involved in reactions (1) and (4) to produce gluconate from glucose and xylonate from xylose, respectively, 6 the number of electrons involved in reactions (2) and (5) to produce xylonate from glucose and threonate from xylose, respectively, and 10 the number of electrons involved in reaction (3) to produce threonate from glucose.

Because the equation has two unknowns, it cannot be solved. For this reason, two limit configurations are considered: $y = 1$, corresponding to the case where all threonate is formed from xylose, and $y = 0$, corresponding to the case where all threonate is formed from glucose, the reality lying between both these situations. Note that considering the "limit" situations, (i) all carboxylates are formed from glucose oxidation ($x = 0$ and $y = 0$) and (ii) gluconate is formed from glucose oxidation whereas xylonate and threonate are formed from xylose oxidation ($x = 1$ and $y = 1$), and comparing with the electrical charges determined from the chronoamperometric $i(t)$ curves (Figure S11 in Supporting Information) after 6 hours, the faradaic efficiencies were always lower than 1 for "limit" situation (i) and always higher than 1 for "limit" situation (ii) (Table S11 in Supporting Information). The actual faradaic efficiency is then likely close to 1.

The values of x are given in Table 2. These values are always lower than 0.7, which demonstrates that competition between glucose and xylose to react at the $\text{Pd}_{0.3}\text{Au}_{0.7}$ catalytic surface is in favor of glucose for both cell voltages. From the value of x , the actual contribution of xylose oxidation to the formation of products can be determined (Table 2). At +0.4 V, it increases from ca. 3.3 % to ca. 9.4 % ($y = 1$)/12.1 % ($y = 0$), whereas at +0.6 V, it increases from ca. 5.0 % to ca. 34.0 %, for initial xylose proportion increasing from 10 % to 50 %. This fact clearly evidences that glucose is more electro-reactive at the $\text{Pd}_{0.3}\text{Au}_{0.7}$ catalytic surface than xylose, i.e. that glucose has higher affinity than xylose to adsorb at such gold-rich surface, but that the increase of the cell voltage (electrode potential) mitigates this electro-reactivity/affinity difference between both molecules.

Conclusion

Glucose and xylose are the most abundant sugars in lignocellulosic biomass. Their conversion into valuable compounds is then paramount for bioindustries. Electrooxidation is a very interesting mean for this purpose. $\text{Pd}_{1-x}\text{Au}_x/\text{C}$ catalyst are very active for such reaction and selective towards gluconate and xylonate, particularly the $\text{Pd}_{0.3}\text{Au}_{0.7}/\text{C}$ one. Several works investigated the electro-reactivity of pure glucose or xylose solutions. But the conversion of their mixtures, as obtained after lignocellulosic biomass pretreatments to separate lignin from carbohydrates, could allow avoiding the supplementary step of sugar separation.

For the first time, the electro-reactivity of mixtures of these aldoses is studied and we pointed out some aspects on their electrochemical behavior. It was shown from LSVs and *in-situ* infrared spectroscopy measurements that Pd-rich and Au-rich surfaces didn't interact similarly with glucose and xylose, Pd-rich surface favoring the dissociative adsorption of sugar with poisoning of the surface by strongly adsorbed CO species, whereas Au-rich surface avoided the formation of these adsorbates. It was shown that Pd-rich surface displayed higher affinity towards xylose adsorption, whereas Au-rich surface adsorbed preferentially glucose. At last, it was shown from chronoamperometry measurements at different cell voltages and HPLC analyses of the reaction products that glucose was more electro-reactive than xylose at a $\text{Pd}_{0.3}\text{Au}_{0.7}$ surface, and that the increase of the cell voltage mitigates the difference in reactivity between both sugars.

Experimental Section

Chemicals

All chemicals were used as received, except the carbon powder (carbon powder Vulcan XC72 from Cabot Corp.) that underwent a heat treatment at 400 °C under N_2 atmosphere (U-quality from Air Liquide) for 4 hours to remove adsorbed impurities.

For the synthesis of catalysts, potassium tetrachloropalladate and tetrachloroauric acid trihydrate, K_2PdCl_4 and $\text{HAuCl}_4 \cdot 3 \text{H}_2\text{O}$ (99.99% purity), were purchased from Alfa Aesar, n-heptane (99% purity) from Acros Organics, polyethylene glycol dodecyl ether (Brij[®] L4), sodium borohydride (ReagentPlus, 99% purity) and acetone (Chomasolv[®], $\geq 99.8\%$ purity) from Sigma-Aldrich. Ultra-high purity water (18.2 M Ω cm) was obtained from a Milli-Q-Millipore system.

For the electrochemical and spectrochemical measurements, NaOH (semiconductor grade, 99.99% purity), glucose and xylose (99% purity), and Nafion 5 wt. % in aliphatic alcohols were purchased from Sigma-Aldrich.

Synthesis and characterization of catalysts

The synthesis of the $\text{Pd}_{1-x}\text{Au}_x/\text{C}$ catalysts (atomic ratio, $x = 0, 0.3, 0.7$ and 1.0) using a "water in oil" microemulsion method to obtain a metal loading on the carbon support (Vulcan XC72 from Cabot) of 40 wt % was detailed elsewhere¹⁰. A TA (thermo analysis) Instrument model SDT Q 600 was used to determine the metal loading, by gradually heating the

sample from 298 K to 1173 K at a rate of 10 K min⁻¹ under a 100 mL min⁻¹ air flow. The Pd/Au atomic ratios were determined by atomic absorption spectroscopy (AAS) using a Perkin Elmer AA200 Atomic absorption spectrometer. The mean particle sizes were determined from transmission electron microscopy (TEM) images using a JEOL JEM 2100 (UHR) microscope (0.19 nm resolution), whereas the mean crystallite sizes, as well as the microstructure of the catalysts, were determined from X-ray Diffraction (XRD) patterns recorded in the 2 θ range from 20 ° to 90 ° using a PANalytical Empyrean X-ray diffractometer. All the experimental set-ups for the characterization of catalysts are given in reference¹⁰.

Electrochemical and spectro-electrochemical investigations

A Voltalab PGZ402 potentiostat (Radiometer Analytical) was used to record cyclic voltammograms (CVs) and linear sweep voltammograms (LSVs) in a three-electrode cell thermostated at 293 K, fitted with a reversible hydrogen electrode (RHE) as reference and a 3 cm² surface area glassy carbon plate as counter electrode. The preparation of the working electrode is described elsewhere^[10,22]. It consists of depositing Pd_{1-x}Au_x/C catalysts on a 0.0707 cm² glassy carbon disk, with a metal loading of 100 $\mu\text{g}_{\text{metal}} \text{cm}^{-2}$. CVs are recorded in a N₂-purged 0.10 mol L⁻¹ NaOH electrolyte and LSVs in the same electrolyte in the presence of 0.10 mol L⁻¹ glucose/xylose mixtures with molar ratios of 100/0, 90/10, 70/30, 50/50 and 0/100.

A Bruker IFS 66 FTIR (Fourier transform infrared) spectrometer modified for beam reflection on the electrode surface at a 65° incident angle and fitted with an Infrared Associates liquid nitrogen-cooled HgCdTe detector (4 cm⁻¹ resolution) was used to record *in situ* the spectra for the electrooxidation of 0.10 mol L⁻¹ of glucose/xylose mixtures in 0.10 mol L⁻¹ NaOH electrolyte at the surface of the Pd_{1-x}Au_x/C electrodes. The experimental set-up, experimental conditions, and the method for the normalization of spectra are given elsewhere^[10,23]. The method chosen for the normalization of spectra imply that the formation of species/chemical groups led to negative IR absorption bands, whereas the consumption of species led to positive absorption bands.

Electro-reforming of 30 mL of 0.10 mol L⁻¹ glucose/xylose mixtures in 0.10 mol L⁻¹ NaOH electrolytes was performed at 293 K at the constant voltages of +0.4 V and +0.6 V, in a 25 cm² filter-press cell fitted with a Pt/C cathode and a Pt_{1-x}Au_x/C anode (each electrode loaded with 0.5 mg_{metal} cm⁻²) separated by a blotting paper to avoid short-circuit. Every hour for 6 hours a 600 μL aliquot of the anodic solution is sampled to be analyzed by high performance liquid chromatography (Knauer Azura HPLC equipped with a Transgenomic ICSEP COREGEL 107H column) using a UV detector set at $\lambda = 210 \text{ nm}$. The whole experimental set-up was already described elsewhere^{10,18}.

Acknowledgements

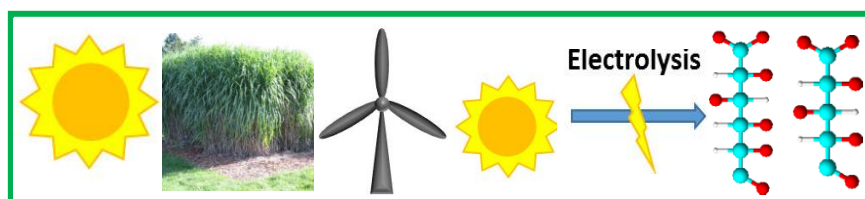
The authors acknowledge the European Union (ERDF), the "Région Nouvelle Aquitaine", the INCREASE research federation (FR CNRS 3707) and the French research agency (ANR) through the Gluconic project (ANR-20-CE43-0005) for financial supports.

Keywords: Glucose • Xylose • electrooxidation • in-situ FTIRS • Electroreforming • Mixture • chronoamperometry

- [1] C. Dolle, N. Neha, C. Coutanceau, *Curr. Opin. Electrochem.* **2022**, *31*, 100841. Doi: 10.1016/j.coelec.2021.100841
- [2] European Innovation Council, EIC Pathfinder challenge: Novel routes to green hydrogen production, can be found under

- https://eic.ec.europa.eu/eic-funding-opportunities/european-innovation-ecosystems/calls-proposals/eic-pathfinder-challenge-2_en, **2021**
- [3] H. Wei, W. Liu, X. Chen, Q. Yang, J. Li, H. Chen, *Fuel* **2019**, *254*, 115599. Doi: 10.1016/j.fuel.2019.06.007
- [4] E. Taarning, C. M. Osmundsen, X. Yang, B. Voss, S. I. Andersen, C. H. Christensen, *Energy Environ. Sci.* **2011**, *4*, 793–804. Doi: 10.1039/c004518g
- [5] V. B. Agbor, N. Cicek, R. Sparling, A. Berlin, D. B. Levin, *Biotechnol. Adv.* **2011**, *29*, 675–685. Doi: 10.1016/j.biotechadv.2011.05.005
- [6] B. Su, D. Song, H. Zhu, *Front. Bioeng. Biotechnol.* **2020**, *8*, 435. Doi: 10.3389/fbioe.2020.00435
- [7] T. Werpy, G. Petersen, A. Aden, J. Bozell, J. Holladay, J. White, A. Manheim, D. Elliot, L. Lasure, S. Jones, M. Gerber, K. Ibsen, L. Lumberg, S. Kelley, Pacific Northwest National Laboratory, National Renewable Energy Laboratory. *Top Value-Added Chemicals from Biomass: Results of Screening for Potential Candidates from Sugars and Synthesis Gas*, Department of Energy, Oak Ridge, TN, **2004**. Doi: 10.2172/15008859
- [8] H. Liu, K.N.G. Valdehuesa, G.M. Nisola, K.R.M. Ramos, W.-J. Chung, *Bioresour. Technol.* **2012**, *115*, 244–248. Doi: 10.1016/j.biortech.2011.08.065
- [9] A. M. Cañete-Rodríguez, I. M. Santos-Dueñas, J. E. Jiménez-Hornero, A. Ehrenreich, W. Liebl, I. García-García, *Process Biochem.* **2016**, *51*, 1891–1903. Doi: 10.1016/j.procbio.2016.08.028
- [10] T. Rafaideen, S. Baranton, C. Coutanceau, *Appl. Catal. B* **2019**, *243*, 641–656. Doi: 10.1016/j.apcatb.2018.11.006
- [11] B. C. Saha, *J. Ind. Microbiol. Biotechnol.* **2003**, *30*, 279–291. Doi: 10.1007/s10295-003-0049-x
- [12] L. Yan, A. Brouzgou, Y. Meng, M. Xiao, P. Tsiakaras, S. Song, *Appl. Catal. B* **2014**, *150–151*, 268–274. Doi: 10.1016/j.apcatb.2013.12.026
- [13] B. Beden, F. Largeaud, K.B. Kokoh, C. Lamy, *Electrochim. Acta* **1996**, *41*, 701–709. doi: 10.1016/0013-4686(95)00359-2.
- [14] A. Zalineeva, S. Baranton, C. Coutanceau, *Electrochim. Acta* **2015**, *176*, 705–717. Doi: 10.1016/j.electacta.2015.07.073. And reference therein.
- [15] Y.-X. Jiang, S.-G. Sun, N. Din, *Chem. Phys. Lett.* **2001**, *344*, 463–470. DOI: 10.1016/S0009-2614(01)00812-0
- [16] J. H. K. Pfisterer, U. E. Zhumaev, W. Cheuquepan, J. M. Feliu, K. F. Domke, *J. Chem. Phys.* **2019**, *150*, 041709. Doi: 10.1063/1.5047941
- [17] A. Dailey, J. Shin, C. Korzeniewski, *Electrochim. Acta* **1998**, *44*, 1147–1152. Doi: 10.1016/S0013-4686(98)00217-5
- [18] N. Neha, B. S. R. Kouamé, T. Rafaideen, S. Baranton, C. Coutanceau, *Electrocatalysis* **2021**, *12*, 1–14. Doi: 10.1007/s12678-020-00586-y
- [19] T. Rafaideen, N. Neha, S. R. B. Kouamé, S. Baranton, C. Coutanceau, *Clean Technol.* **2020**, *2*, 184–203. doi:10.3390/cleantechnol2020013
- [20] M. Tominaga, M. Nagashima, K. Nishiyama, I. Taniguchi, *Electrochem. Commun.* **2007**, *9*, 1892–1898. Doi:10.1016/j.elecom.2007.04.024
- [21] C. Lamy, C. Coutanceau, S. Baranton, *Production of clean hydrogen by the electrochemical reforming of oxygenated organic compounds*, in *Hydrogen and Fuel cells primers*, (Ed.: B. Pollet), Elsevier, Amsterdam, **2020**, pp 9-20. ISBN: 978-0-12-821500-5
- [22] B. S. R. Kouamé, S. Baranton, P. Brault, C. Canaff, W. Chamorro-Coral, A. Caillard, K. De Oliveira Vigier, C. Coutanceau, *Electrochim. Acta* **2019**, *329*, 135161. Doi: 10.1016/j.electacta.2019.135161
- [23] M. Simoes, S. Baranton, C. Coutanceau, *ChemSusChem* **2012**, *5*, 2106–2124. Doi: 10.1002/cssc.201200335

Entry for the Table of Contents



After separation of lignin from lignocellulosic biomass, glucose and xylose are the main sugars remaining in hydrolysates. The selective electroreforming of glucose/xylose mixtures into their corresponding carboxylates is studied for the first time. Results from linear scan voltammetry, *in-situ* infrared spectroscopy and chronoamperometry measurements give new insights on the reactivity of both sugars at a Pd₃Au₇ catalytic surface.